Influence of Structural Design on the Aeroelastic Stability of Brancusi's Endless Column

R. D. Gabbai[1]

Abstract: Brancusi's Endless Column (Târgu-Jiu, Romania) is an interesting case study in bluff body aeroelasticity. It has been referred to as aeroelastically indifferent owing to its remarkable aeroelastic stability. This stability has been attributed to its unconventional shape. Calculations are presented which show that this strictly aerodynamic view of the column behavior is incomplete, and that the structural dynamics characteristics of the column have a powerful role in ensuring its aeroelastic stability. The calculations show that the column's design, which provided for significant damping and mass, would assure its aeroelastic stability even if the column had a conventional and aeroelastically less favorable shape, i.e., if it were a circular cylinder (a shape that is unfavorable from the point of view of vortex-induced response) or a square cylinder (a shape that is unfavorable from the point of view of galloping).

DOI: 10.1061/(ASCE)0733-9399(2008)134:6(462)

CE Database subject headings: Aeroelasticity; Vortex shedding; Wind loads; Structural engineering; Columns.

Introduction

Brancusi's Endless Column (EC) (Fig. 1) is an interesting case study in bluff body aeroelasticity. Because is has remarkably aeroelastic stability it has been called "aeroelastically indifferent." The EC has been the subject of a number of landmark experimental studies that had as their motivation the characterization of its aeroelastic response (e.g., Lungu et al. 2002). The column's aeroelastic behavior has been attributed to its unconventional shape. It is shown here that the column's *structural* design is at least as important in assuring its aeroelastic stability with respect to both vortex shedding and galloping. The design provided for sufficiently large damping and mass, which would have assured aeroelastic stability even if the column had a conventional and aeroelastically less favorable shape, e.g., a circular or square cylinder.

Cylindrical towers with a circular cross section exhibit vortex-induced response. The Basu and Vickery procedure (1983a) (also see Chap. 10 of Simiu and Scanlan 1996) is applied to show that such a cylindrical tower, with the same dimensions and mechanical properties as the EC, has negligible vortex-induced response, in spite of its aerodynamically unfavorable shape.

Cylinders with circular cross section do not gallop (Simiu and Scanlan 1996, p. 234). When examining galloping, a tower is considered whose dimensions and mechanical properties are the same as the EC, but whose cross section is square and hence more unfavorable aeroelastically. Owing to its damping and mass, this tower also has negligible galloping response.

[1]NIST/NRC Postdoctoral Research Associate, Building and Fire Research Laboratory, National Institute of Standards and Technology, Gaithersburg, MD 20899-8611. E-mail: rdgabbai@gmail.com

Note. Associate Editor: Kuang-An Chang. Discussion open until November 1, 2008. Separate discussions must be submitted for individual papers. To extend the closing date by one month, a written request must be filed with the ASCE Managing Editor. The manuscript for this paper was submitted for review and possible publication on February 20, 2007; approved on October 18, 2007. This paper is part of the ***Journal of Engineering Mechanics***, Vol. 134, No. 6, June 1, 2008. ©ASCE, ISSN 0733-9399/2008/6-462–465/$25.00.

Vortex-Induced Vibration

The EC height is $L=29.35$ m. Its plane cross sections are square with 0.45–0.90 m sides.

No procedures appear to have been developed for estimating the vortex-induced response of towers with the shape of the EC or for towers with square cross section in atmospheric flows. However, such a procedure has been developed by Basu and Vickery (1983a,b) and Vickery and Basu (1983) for circular cylinders. The mechanical properties of the circular column used in that procedure are listed in Table 1. The critical wind speed for vortex-induced vibration corresponding to the first normal mode of vibration has the expression

$$V_{01_{\mathrm{cr,vs}}} = \frac{\omega_1 D}{2\pi S}, \tag{1}$$

where S=Strouhal number; D=diameter; and $V_{01_{\mathrm{cr,vs}}}$ velocity at which the Strouhal circular frequency for the stationary column, $\omega_s = 2\pi S V_0 / D$=first natural circular frequency of the system ω_1. Assuming $S=0.20$ (Simiu and Miyata 2006, p. 191), the critical wind speed corresponding to each diameter can be readily computed from Eq. (1). The results are shown in the second column of Table 2. The Reynolds number for each $V_{01_{\mathrm{cr,vs}}}$ is

$$\mathcal{R} = (6.7 \times 10^4) V_{01_{\mathrm{cr,vs}}} D \tag{2}$$

where D is in m and $V_{01_{\mathrm{cr,vs}}}$ is in m/s. The values of $\mathcal{R}$ so determined are also listed in Table 2.

The response depends on the RMS lift coefficient $\overline{C_L^2}^{1/2}$, the spanwise correlation parameter $\mathcal{L}$, and the aeroelastic parameter K_{a0} (1) (see Basu and Vickery 1983a). These are functions of $\mathcal{R}$ and are shown in Table 3. The procedure yields the RMS deflection $\sigma_{y1}(L)$ and the peak deflection $Y_1(L)$ (Table 4). The peak factor g_{y1} that multiplies $\sigma_{y1}(L)$ to yield the peak response $Y_1(L)$ is independent of D and has the approximate value 4.0.

Tables 3 and 4 show that: (1) the critical velocity for vortex-induced vibration, $V_{01_{\mathrm{cr,vs}}}$, is on the order of 1 m/s; and (2) the peak deflections are negligible.

Table 5. Analysis Cases

Case number	D (m)	V_0 (m/s)	Flow type
I	0.45	19–204	Smooth
II	0.45	19–210	Boundary layer
III	0.675	12–136	Smooth
IV	0.675	13–140	Boundary layer
V	0.90	9–102	Smooth
VI	0.90	9–105	Boundary layer

resonance occurs (Parkinson and Smith 1964; Vio et al. 2004). As is shown in Table 7 (see Table 2), this is true in the present case.

The profile of the incoming flow, $V(z)$, is defined by either

$$V(z)=\begin{cases} V_0, & \text{smooth flow} \\ V_0\left(\dfrac{z}{L}\right)^{1/7}, & \text{boundary layer flow} \end{cases} \tag{3}$$

Both profiles are considered in the analysis. The analysis cases are summarized in Table 5.

The three different values of D represent the minimum (0.45 m), the average (0.675 m), and the maximum (0.90 m) side of the square horizontal cross sections of each of the 16 cast iron modules (the "beads") of height 1.80 m that form the outermost part of the column.

The relevant mechanical and dynamic properties of the EC model are listed in Table 1. Because the response is dominated by the first mode of vibration, only that mode is considered in the analysis. The mass per unit length with axial height $\mu(z)$ is shown in Table 6.

Using the data in Table 6, the value of the generalized mass M_1 is obtained as follows

$$M_1=\int_0^L \mu(z)\psi_1^2(z)dz$$

$$=1{,}525\int_0^{0.56}\left(\frac{z}{L}\right)^4 dz+\cdots+486\int_{28.90}^{29.35}\left(\frac{z}{L}\right)^4 dz \tag{4}$$

The expression for the critical velocity for galloping oscillation in the first mode is given by

$$V_{01_{cr,g}}=\frac{4\zeta_1\omega_1 M_1}{\rho D A_1 \hat{c}_{1_1}} \tag{5}$$

or, in terms of the reduced velocity **

$$U_{01_{cr,g}}=\frac{4\zeta_1 M_1}{\rho D^2 A_1 \hat{c}_{1_1}} \tag{6}$$

where $\rho\approx 1.25$ kg/m^3, $A_1=2.69$, and $\hat{c}_{1_1}$ is defined by Eq. (7)

Table 6. Distribution of Mass

Range (m)	$\mu(z)$ (kg/m)
$0\le z\le 0.56$	1,525
$0.56<z\le 5.50$	1,261
$5.50<z\le 9.36$	1,005
$9.36<z\le 20.42$	752
$20.42<z\le 28.90$	608.5
$28.90<z\le 29.35$	486

Table 7. Critical Galloping Velocity $V_{01_{cr,g}}$ for Each Case

Case number	$V_{01cr,g}$ (m/s)
I	92.9
II	95.6
III	61.9
IV	63.7
V	46.5
VI	47.8

$$\hat{c}_{1_1}=\frac{1}{V_0}\int_0^L V(z)\left(\frac{z}{L}\right)^4 dz \tag{7}$$

For each analysis case, the range of U_{01} was specified as $0.2U_{01_{cr,g}}\le U_{01}\le 2.2U_{01_{cr,g}}$. Since $U_{01_{cr,g}}$ is a function of both D and $\hat{c}_{1_1}$ [see Eq. (6)], the corresponding range of the mean wind speed V_0 is in each case different. These differences are shown in the third column of Table 5. Table 7 lists the critical onset velocity for galloping for each case considered.

Figs. 2(a–c) show the maximum transverse displacement at the beam tip $y_1(L)$ for each case as a function of V_0. It is apparent that the effect of the shear flow is to retard the onset velocity of galloping, albeit only slightly in this case. This is consistent with the experimental observations recorded in Novak (1972).

It is clear from the figures that the cantilevered square section model of the EC is not susceptible to galloping for any of the cases considered if the mean velocity at the top of the building is less than about 47 m/s, or about $47(10/29.35)^{1.7}=49.3$ m/s at 10 m above ground in open terrain. (The latter value corresponds to a 3 s gust speed of about 74.9 m/s.) It is unlikely that such speeds would occur in Târgu-Jiu, Romania, the site of the actual Endless Column.

The galloping velocity for the square column in the most unfavorable case (D=0.90 m) is large owing to the relatively high damping (1.75%) and generalized mass in the fundamental mode of vibration (M_1=3,661 kg). The coefficients in the expression for the aerodynamic galloping excitation correspond to smooth flow. Their use for the modeling of galloping under turbulent flow is conservative (Novak 1972), that is, it yields onset galloping velocities somewhat smaller than those that would actually occur in turbulent flow.

Conclusions

The aim of this paper is to elaborate on an aspect of the aeroelastic behavior of the Brancusi EC that has not been given much attention in previous engineering studies. It has been pointed out in the literature that the EC is characterized by aerodynamic parameters resulting in favorable aeroelastic behavior. It was shown in the paper that the column's favorable aeroelastic behavior is assured, in addition, by the large values of its structural dynamics parameters—the damping and the mass—provided for by Brancusi's structural engineer, Stefan Georgescu-Gorjan. Had the column consisted of a circular or square cylinder, its aeroelastic behavior would have been excellent as well.

Acknowledgments

The writer performed this work during his tenure as an NIST-NRC Postdoctoral Research Associate. The advice of his advisor, Dr. Emil Simiu, is gratefully acknowledged.

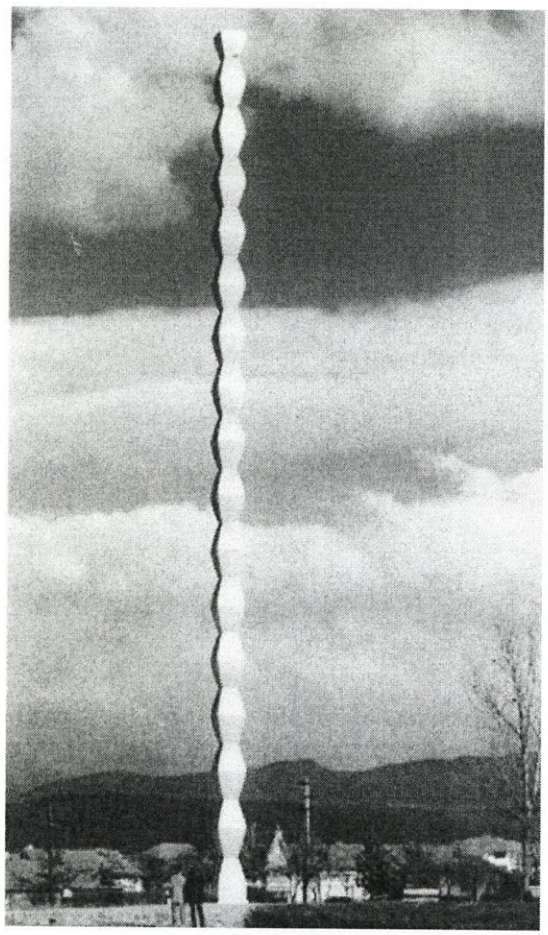

Fig. 1. (Color) Endless column by Constantin Brancusi, Târgu-Jiu, Romania. (Reprinted with permission of World Monuments Fund, which oversaw restoration project of column.)

It is important to point out that the writer also investigated the vortex-induced response in the second normal mode of vibration using the procedure described above. For each value of the diameter D considered, approximate calculations of the peak deflections at the top of the column of in the second mode of vibration were based on: (1) the modal analysis of a uniform cantilever (Meirovitch 1986, p. 163); and (2) the aerodynamic parameter values (Basu and Vickery 1983a) corresponding to the Strouhal number (and thus to the Reynolds number). The results indicate

Table 1. Mechanical and Dynamic Properties of EC Model

Parameter	Symbol	Value
Damping ratio[a,b]	ζ_1	0.0175
Circular natural frequency[a,b]	ω_1	3.22 rad/s
First normal mode	$\psi_1(z)$	$(z/L)^2$
Generalized mass[a,b]	M_1	3,661 kg
Reduced velocity[a]	U_{01}	$V_0/\omega_1 D$

[a]Subscript 1 indicates that the parameter corresponds to the first normal mode.

[b]Values obtained through the courtesy of Dr. M. Iancovici from Dr. R. Vacareanu of the Technical University of Civil Engineering, Bucharest, Romania.

Table 2. Critical Velocity for Vortex Induced Vibration and Corresponding Reynolds Number as Function of Cylinder Diameter

D (m)	$V_{01_{cr,vs}}$ (m/s)	$\mathcal{R}$
0.45	1.15	3.47×10^4
0.675	1.72	7.78×10^4
0.90	2.30	1.39×10^5

that for a given value of D, the peak response $Y_2(L)$ in the second mode of vibration is slightly less than its counterpart in the first mode of vibration $Y_1(L)$. This in spite of the fact that the critical velocity for vortex shedding excitation $V_{02_{cr,vs}}$ is larger than $V_{01_{cr,vs}}$.

Galloping

In the previous section, the response of the EC to vortex excitation was estimated by assuming, conservatively, aerodynamic properties associated with a more unfavorable shape, the circular cylinder. As was mentioned earlier, cylindrical shapes with circular cross section do not gallop, and a tower with the same dimensions and mechanical properties as the EC, but with the shape of a cylinder with square cross section, is considered. The susceptibility of this shape to galloping is well established (Parkinson and Smith 1964; Novak 1972). Even though, as can be inferred from data available in Mukhopadhyay and Dugundji (1976) and Lungu et al. (2002), this shape is aerodynamically more unfavorable than the shape of the EC, it is shown here that owing to its relatively large damping and mass, the tower would exhibit negligible galloping response.

The model being considered then consists of a vertical cantilevered beam of constant square cross section and variable mass per unit length $\mu(z)$. The galloping response of the cantilever beam in the first mode of vibration can be estimated by solving numerically a single degree-of-freedom equation of motion with damping modeled by a seventh-degree polynomial term with odd powers (Vio et al. 2004). The nonlinear terms are introduced when the aerodynamic force is modeled using the quasi-steady approximation for the transverse force. The quasi-steady theory is generally considered to be valid as long as the critical velocity is at least four times higher than the critical velocity at which vortex

Table 3. Aerodynamic and Aeroelastic Parameters

D (m)	$\overline{C_L^2}^{1/2}$	$\mathcal{L}$	K_{a0} (1)[a]
0.45	0.45	2.5	2.18
0.675	0.45	2.5	2.18
0.90	0.45	2.5	1.21

[a]Values based on a roughness length $z_0=0.05$ m, and a relative surface roughness on the cylinder of $k/D=1\times10^{-4}$.

Table 4. RMS of Deflection $\sigma_{y1}(L)$ and Peak Deflection $Y_1(L)$

D (m)	$\sigma_{y1}(L)$ (m)	$Y_1(L)$ (m)
0.45	2.44×10^{-4}	9.76×10^{-4}
0.675	1.04×10^{-3}	4.16×10^{-3}
0.90	2.90×10^{-3}	1.16×10^{-2}

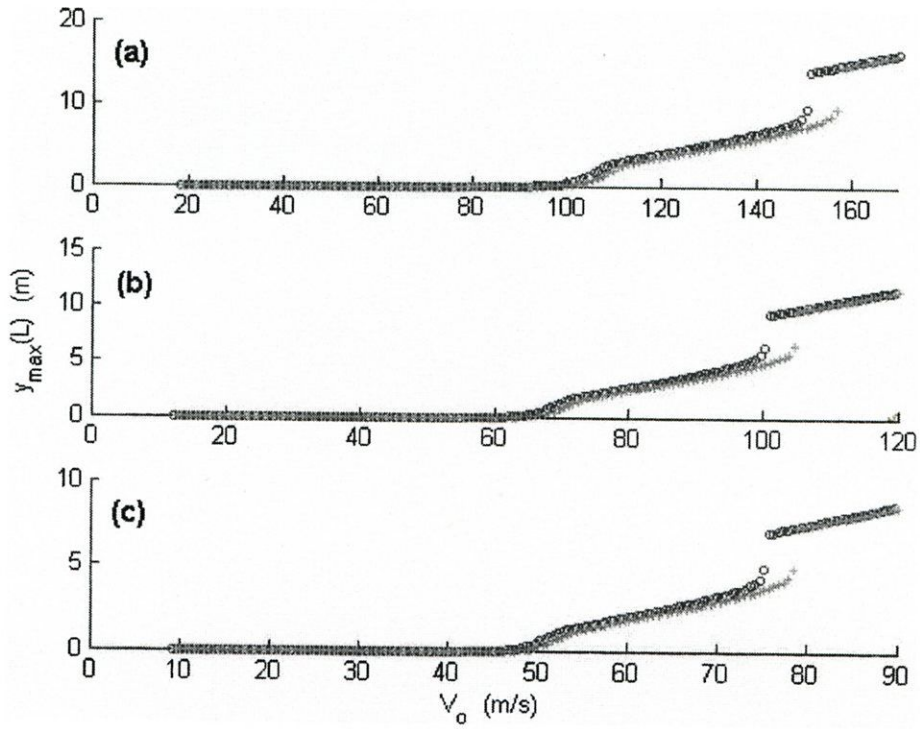

Fig. 2. (Color) Galloping response for: (a) $D=45$ cm (Cases I and II); (b) $D=67.5$ cm (Cases III and IV); and (c) $D=90$ cm (Cases V and VI). In all cases, (◦) represents smooth flow and (+) represents boundary layer flow.

References

Basu, R. I., and Vickery, B. J. (1983a). "Across wind vibrations of structures of circular cross- section. Part 2: Development of a mathematical model for full-scale application." *J. Wind. Eng. Ind. Aerodyn.*, 12(1), 75–97.

Basu, R. I., and Vickery, B. J. (1983b). "Simplified approaches to the evaluation of across-wind response of chimneys." *J. Wind. Eng. Ind. Aerodyn.*, 14(1–3), 153–166.

Lungu, D., Solari, G., Bartoli, G., Righi, M., Vacareanu, R., and Villa, A. (2002). "Reliability under wind loads of the Brancusi Endless Column, Romania." *Int. J. Fluid Mech. Res.*, 29(3–4), 323–328.

Meirovitch, L. (1986). *Elements of vibration analysis*, McGraw-Hill, New York.

Mukhopadhyay, V., and Dugundji, J. (1976). "Wind excited vibration of a square section cantilever beam in smooth flow." *J. Sound Vib.*, 45(3), 329–339.

Novak, M. (1972). "Galloping oscillations of prismatic structures." *J. Engrg. Mech. Div.*, 98(1), 27–46.

Parkinson, P., and Smith, J. D. (1964). "The square prism as an aeroelastic non-linear oscillator." *Q. J. Mech. Appl. Math.*, 17(2), 225–239.

Simiu, E., and Miyata, T. (2006). *Design of buildings and bridges for wind*, Wiley, Hoboken, N.J.

Simiu, E., and Scanlan, R. H. (1996). *Wind effects on structures*, Wiley, New York.

Vickery, B. J., and Basu, R. I. (1983). "Across wind vibrations of structures of circular cross-section. Part 1: Development of a mathematical model for two-dimensional conditions." *J. Wind. Eng. Ind. Aerodyn.*, 12(1), 49–73.

Vio, G. A., Dimitriadis, G., and Cooper, J. E. (2004). "On the solution of the aeroelastic galloping problem." *Proc. Int. Conf. on Noise and Vibration Engineering (ISMA 2004)*, P. Sas and M. De Munck, eds., Katholieke Universiteit Leuven, Leuven, Belgium, 2211–2226.